insects

MDPI

Article

Seasonal Phenology and Climate Associated Feeding Activity of Introduced *Marchalina hellenica* in Southeast Australia

Duncan D. Jaroslow [1,*], John P. Cunningham [2,3], David I. Smith [4,5,6] and Martin J. Steinbauer [1]

[1] Department of Ecology, Environment and Evolution, La Trobe University, Melbourne, VIC 3086, Australia
[2] School of Applied Systems Biology, La Trobe University, Melbourne, VIC 3086, Australia
[3] Agriculture Victoria, AgriBio Centre for AgriBioscience, Melbourne, VIC 3086, Australia
[4] Agriculture Victoria, Biosecurity and Agricultural Services, Cranbourne, VIC 3977, Australia
[5] School of Ecosystem and Forest Sciences, University of Melbourne, Parkville, Burnley, VIC 3121, Australia
[6] ArborCarbon, Murdoch University, Murdoch, WA 6150, Australia
* Correspondence: duncan.jaroslow@latrobe.edu.au

Simple Summary: Giant pine scale, *Marchalina hellenica* Gennadius (Hemiptera, Marchalinidae), is a sap sucking insect native to the Eastern Mediterranean Basin. In 2014, giant pine scale was detected for the first time in Victoria, Australia, feeding on a new host, *Pinus radiata*. We studied the life cycle and feeding activity of giant pine scale in Victoria over 32 months, with the aim of drawing comparisons between exotic and native populations. Australian life stages of this pest emerged during similar months to Greek seasonal equivalents, although the timing of Australian life stages differed between years. Insect density and feeding activity on infested trees differed among locations and between generations. Strong evidence was found in support of density and feeding intensity being explained by climatic conditions. The value of *Pinus radiata* as a food source for this insect may fluctuate with climate conditions. Our findings aim to inform future management efforts for this scale insect, including surveillance strategies and optimal seasons for release of biocontrol agents. Our findings also suggest that the impact of this pest in Australia may be exacerbated by climate change.

Abstract: Invasive insects pose an increasing risk to global agriculture, environmental stability, and public health. Giant pine scale (GPS), *Marchalina hellenica* Gennadius (Hemiptera: Marchalinidae), is a phloem feeding scale insect endemic to the Eastern Mediterranean Basin, where it primarily feeds on *Pinus halepensis* and other Pinaceae. In 2014, GPS was detected in the southeast of Melbourne, Victoria, Australia, infesting the novel host *Pinus radiata*. An eradication program was unsuccessful, and with this insect now established within the state, containment and management efforts are underway to stop its spread; however, there remains a need to understand the insect's phenology and behaviour in Australia to better inform control efforts. We documented the annual life cycle and seasonal fluctuations in activity of GPS in Australia over a 32 month period at two contrasting field sites. Onset and duration of life stages were comparable to seasons in Mediterranean conspecifics, although the results imply the timing of GPS life stage progression is broadening or accelerating. GPS density was higher in Australia compared to Mediterranean reports, possibly due to the absence of key natural predators, such as the silver fly, *Neoleucopis kartliana* Tanasijtshuk (Diptera, Chamaemyiidae). Insect density and honeydew production in the Australian GPS population studied varied among locations and between generations. Although insect activity was well explained by climate, conditions recorded inside infested bark fissures often provided the weakest explanation of GPS activity. Our findings suggest that GPS activity is strongly influenced by climate, and this may in part be related to changes in host quality. An improved understanding of how our changing climate is influencing the phenology of phloem feeding insects such as GPS will help with predictions as to where these insects are likely to flourish and assist with management programs for pest species.

Keywords: seasonal phenology; phloem-feeders; insect density; honeydew; climate drivers

Citation: Jaroslow, D.D.; Cunningham, J.P.; Smith, D.I.; Steinbauer, M.J. Seasonal Phenology and Climate Associated Feeding Activity of Introduced *Marchalina hellenica* in Southeast Australia. *Insects* **2023**, *14*, 305. https://doi.org/10.3390/insects14030305

Academic Editors: Francesco Parisi, Klaus H. Hoffmann, Enrico Ruzzier and Simone Sabatelli

Received: 28 February 2023
Revised: 14 March 2023
Accepted: 17 March 2023
Published: 21 March 2023

1. Introduction

Invasive insects pose a serious threat to forest health, ecosystem stability, and even public health in areas where they establish [1–4]. Field observations of an exotic insect's life cycle can be important to understanding their population dynamics in the new environment and when control efforts could be maximised [5,6]. This would be particularly important for understanding species establishing in both the northern and southern hemispheres, due to the inverse of calendar season. Phenological studies might include documenting insect activity patterns and emergence of developmental stages (e.g., [7,8]) and, in the case of herbivorous insects, matching these to fluctuations in host quality [9,10]. For phloem feeding insects, mapping the timing of feeding life stages and feeding activity can be used to predict when impacts are greatest [11–13]. In Australia, insect forest pests are being detected at an accelerating rate [14,15], many of which are phloem-feeding insects.

In 2014, the giant pine scale, *Marchalina hellenica* Gennadius, (Hemiptera, Marchalinidae) was first detected in Victoria, Australia, feeding on the novel host *Pinus radiata*, or California Monterey pine [16]. *Marchalina hellenica* is endemic to the eastern Mediterranean basin [17–19]; its establishment on *P. radiata* (which originates from North America) poses a significant threat to Australian softwood plantations. *Pinus radiata* represents the vast majority of Australia's more than 1 million hectares of softwood plantation [20]. Despite the widespread use of *P. radiata* as a plantation species and an ornamental, in public gardens and farm windrows, across Australia, the documented distribution of *M. hellenica* is currently restricted to southeast Melbourne [16].

Little is known about how the life cycle of *M. hellenica* in its new Australian habitat compares to its endemic range. The insect's three immature nymphal instars acquire nutrients for development from the sap of pine trees [21]. The nymphal instars feed on phloem by inserting syringe-like stylets into twigs, branches, trunks, and exposed roots [22–24]. As with many phloem-feeding insects, excess carbohydrates and undesirable compounds such as insecticides [25] that are ingested must be excreted as honeydew [26,27]. *Marchalina hellenica* does not feed on host trees all year round, and only the nymphal instar stages possess a functioning stylet and produce honeydew [28]. *Marchalina hellenica* likely originates from Mount Carmel in Northern Israel, the origin of its primary host, *P. halepensis* [29]. Honeydew produced by *M. hellenica* is collected by honeybees across the Eastern Mediterranean and accounts for 60% (~15,000 tonnes) of annual honey produced in Greece [30,31]. While this is important for apiculture in Greece, it also highlights the phloem feeding capability of this insect. Its impact as an introduced pest to Australian forestry could be severe, particularly if feeding stages are prolonged and/or populations flourish in the absence of important native predators, such as the predatory fly, *Neoleucopis kartliana* Tanasijtshuk (Diptera: Chamaemyiidae) [32]. In addition to exuding honeydew, *M. hellenica* secretes cotton-like wax filaments [21] termed flocculent, which may provide a hydrophobic layer and microclimate to protect scales from desiccation and flooding of feeding sites [33–35].

Insect density and availability of honeydew are key indicators of the resources expropriated by *M. hellenica*. Explaining variation in these indicators is important for understanding the insect's activity patterns. As an ectothermic phloem feeder, *M. hellenica* activity is likely related to climate via effects on host nutritional quality [36,37]. As an insect sheltering under bark and flocculent, climate conditions directly experienced by *M. hellenica* may therefore provide inferior explanations for variation in insect activity than the climate experienced by host plants [9,38]. Understanding how *M. hellenica* responds to the climate may help predict the potential spread of this pest in Australia or the impact as the climate in the Mediterranean [39,40] and Pacific region [41,42] trend towards more unpredictable conditions through climate change.

In this study, we used field-sampling to document the seasonal phenology of *M. hellenica* in southeast Melbourne, Victoria, across two and a half insect generations. As these represent the only known *M. hellenica* populations in the southern hemisphere or outside Europe, we explored whether major life cycle milestones (e.g., nymph emergence

or moults) in Melbourne aligned with equivalent seasonal periods to East-Mediterranean conspecifics (i.e., 6 calendar-month difference). We also investigated whether the timing of instar stages and honeydew production (as the proportion of honeydew producing insects, HPI) followed the same seasonal pattern as Mediterranean conspecifics. As a univoltine (one generation per year) and semelparous (mortality following oviposition) insect, density of *M. hellenica* was predicted to reach the generational minimum during the adult stage and maximum at nymph emergence. Finally, we explored the prediction that variation in *M. hellenica* activity would be best explained by the environmental conditions experienced by the host tree, rather than the conditions directly experienced by *M. hellenica*.

2. Materials and Methods

2.1. Study Sites

Infested *M. hellenica* branches were collected every second week (fortnightly) from January 2019 to October 2021, or weekly during moulting periods, from two field sites in south-east Melbourne, Australia: Cardinia Reservoir Park (CRP) in Cardinia (managed by Parks Victoria, a government agency of the state of Victoria, Australia) (37°58′1.5″ S, 145°23′41.4″ E), and Dalton Reserve (DR) in Harkaway (managed by City of Casey Council) (38°0′8.3″ S, 145°20′35.2″ E). Insects were considered to be in a moulting period when more than one life stage was concurrently detected.

The two field sites were selected due to (i) the reliable accessibility, (ii) trees not being removed during the three-year survey period, and (iii) differences in habitat structure, specifically tree density and size. *Pinus radiata* trees at CRP were planted in 1973 to help stabilise soil around the reservoir's banks [43]. The stands of *M. hellenica* infested *P. radiata* were planted in plantation style rows and are of a fairly uniform age. The understory is smothered in dead *P. radiata* needles, with little to no grass or other ground-covering vegetation and an open mid-story consisting of native *Pittosporum undulatum*. Forest surrounding these *P. radiata* stands were dominated by *Eucalyptus* and *Acacia* species. By contrast, DR is a small publicly accessible park located in Harkaway. There are only a handful of ornamental *P. radiata* at DR, all of which were found to be infested. The DR pine trees were much larger than those sampled at CRP. The ground of this reserve is covered by introduced grasses. Other large ornamental trees are present, such as *Eucalyptus leucoxylon* and *Acacia mearnsii*; the canopies of *P. radiata* and other trees at DR do not form a closed canopy.

2.2. Environmental Conditions

Local temperature and relative humidity (RH %) at CRP were recorded using data loggers (accurate to 1.0 °C and resolved to 0.125 °C; DS1923, iButton®, Whitewater, WI, USA). At each site, a data logger was either affixed to the surface of an infested tree trunk (exposed) or wedged into a *P. radiata* bark fissure and under naturally present flocculent, where sufficient flocculent was present to shelter the data logger (fissure) as close to 1.5 m above the south-facing base of the tree as feasible. Data loggers recorded temperature and relative humidity every 30 min, with the exception of a few recordings missed during monthly data retrieval and logger resets. Vapour pressure deficit (VPD), recorded in kPa, was calculated from temperature and relative humidity via an established adaptation of the Magnus equation for vapour saturation point [44–46]. Exposed records were recorded over 707 days (1 November 2019–7 October 2021) and bark fissure records over 469 days (26 June 2020–7 October 2021).

Temperature (°C) and solar exposure (MJ m^{-2}) records were sourced from the Bureau of Meteorology and recorded at Ferny Creek weather station [47]. The Bureau of Meteorology sourced records are referred to here as 'ambient' climate variables. Daily rainfall (mm) was sourced from Melbourne Water [48] and recorded in Emerald, which was closer to field sites than Ferny Creek weather station and at a similar elevation. Rainfall, solar exposure, and ambient temperature records span the entirety of the honeydew and density data; 934 days (19 March 2019–7 October 2021). This also allowed temperature from iButtons

to be compared with ambient temperatures captured by weather stations. Daily climate maximums were converted to fortnightly means for analyses. Rainfall was recorded as cumulative rainfall per fortnight.

The three climate record types covered different temporal ranges. To better compare climate record type, ambient and exposed climate recordings were truncated to match the time period recorded by fissure records (26 June 2020–7 October 2021; 469 days).

2.3. Seasonal Phenology

Seasonal phenology was documented at a minimum interval of fortnightly from January 2019 to October 2021. *Pinus radiata* infested with *M. hellenica*, since December 2018, at each field site were recorded. *Pinus radiata* trees were randomly selected for sample collection through a series of dice rolls. *P. radiata* were excluded from this random selection if their stem diameter was less than 50 cm or if branches were not accessible from ground-level. Sampled *P. radiata* at CRP were approximately 75-metres apart and 140-metres apart at DR, meaning the foliage of these trees at each site did not touch. Excised branches were collected from two trees infested with *M. hellenica* at each site across the study period. Samples were limited to two samples of 30 cm of infested branches per tree per week, with a diameter from 0.5 cm to 2 cm. Infested branches were those that had fresh flocculent or wandering adults (for September to October). Lengths of 9 cm to 11 cm subsections of infested pine twigs and *M. hellenica* were inspected in the laboratory under a dissection microscope (Wild M3Z, Wild Heerbrugg, Heerbrugg, Canton of St. Gallen, Switzerland) (Figure 1) and illuminated using a halogen gooseneck lamp (KL 2500 LED, Leica, Wetzlar, Hesse, Germany). Surface area of sampled twigs, calculated from twig length and diameter, was used to determine the density of *M. hellenica*, expressed as *M. hellenica* per square centimetre (GPS [cm^{-2}]) [49].

The developmental stage of *M. hellenica* present on host material was determined based on a combination of antennal segment count, presence of body setae or dermal spines, and sclerotized body part size (key to *M. hellenica* life stages: [28]). Life stages were identified as honeydew producing insects (HPI) via visual confirmation of the presence of honeydew after lightly squeezing their abdomen [50]. The number of HPI was converted to a percentage of the sampled population of *M. hellenica* (HPI %). To account for combined variation in GPS [cm^{-2}] and HPI [%], GPS [cm^{-2}] was multiplied by HPI [%] to obtain the density of honeydew producing insects, expressed as HPI [cm^{-2}]. This was used as an estimation of the density of *M. hellenica* producing honeydew, accounting for the decline in GPS [cm^{-2}] as each generation progresses [51] and seasonal fluctuations in HPI [%] [50]. Honeydew was collected from HPI from each phenological sample. When less than 10 HPI were available, all HPI were recorded. During the honeydew squeeze test of these HPI subsets, any honeydew was collected using microcapillary tubes of known volume, enabling honeydew volume (HV µL) to be calculated. GPS [cm^{-2}], HPI [%], HPI [cm^{-2}], and HV [µL] values were converted to fortnightly means for each field site. For GPS [cm^{-2}], 61 fortnightly samples for CRP and 50 for DR were retained for analysis. CRP had 49 and DR had 44 HPI [%] fortnights sampled, allowing HPI [cm^{-2}] to be calculated across 49 and 44 fortnights for CRP and DR, respectively. CRP had 26 and DR had 27 fortnights sampled for mean HV [µL].

2.4. Statistical Analysis

Statistical analyses were carried out in SPSS (version 28.0.1.0, IBM Corp., Armonk, NY, USA; access provided by La Trobe University: Department of Ecology, Environment and Evolution; $\alpha = 0.05$) [52]. Life cycle milestones for recorded generations were reported descriptively, including the first detection of each life stage within generations. The proportions of instar, adult, and egg stages represented in sampled populations were plotted over time, with HPI % overlayed to facilitate visual interpretation of *M. hellenica* phenology in relation to honeydew availability [50,53]. Maximum and minimum values for GPS [cm^{-2}], HPI [%], HPI [cm^{-2}], and HV [µL] were reported across *M. hellenica* generation

and collection sites. Pearson's correlation was used to determine which instar stage had the strongest correlation with HPI [%]. Fortnightly means of insect density across both CRP and DR were grouped by calendar month, which were then compared for differences in GPS [cm^{-2}] via Kruskal–Wallis Test of Independent Samples (KW). Differences between specific months included in KW were compared for temporal differences via Dunnett's all-pairs comparison test (Dunnett T3). Dunnett T3 is a non-parametric post-hoc test, and thus, does not assume equal distribution or variance among groups [54]. Dunnett T3 was unable to resolve differences in insect density between any month-based groups. To indicate which months were most dissimilar, the Tukey's Honestly Significant Differences (Tukey's HSD) post-hoc test was used to explore differences in density between months [55], although Tukey's HSD outcome must be interpreted with caution (Tukey's HSD assumes data are parametric).

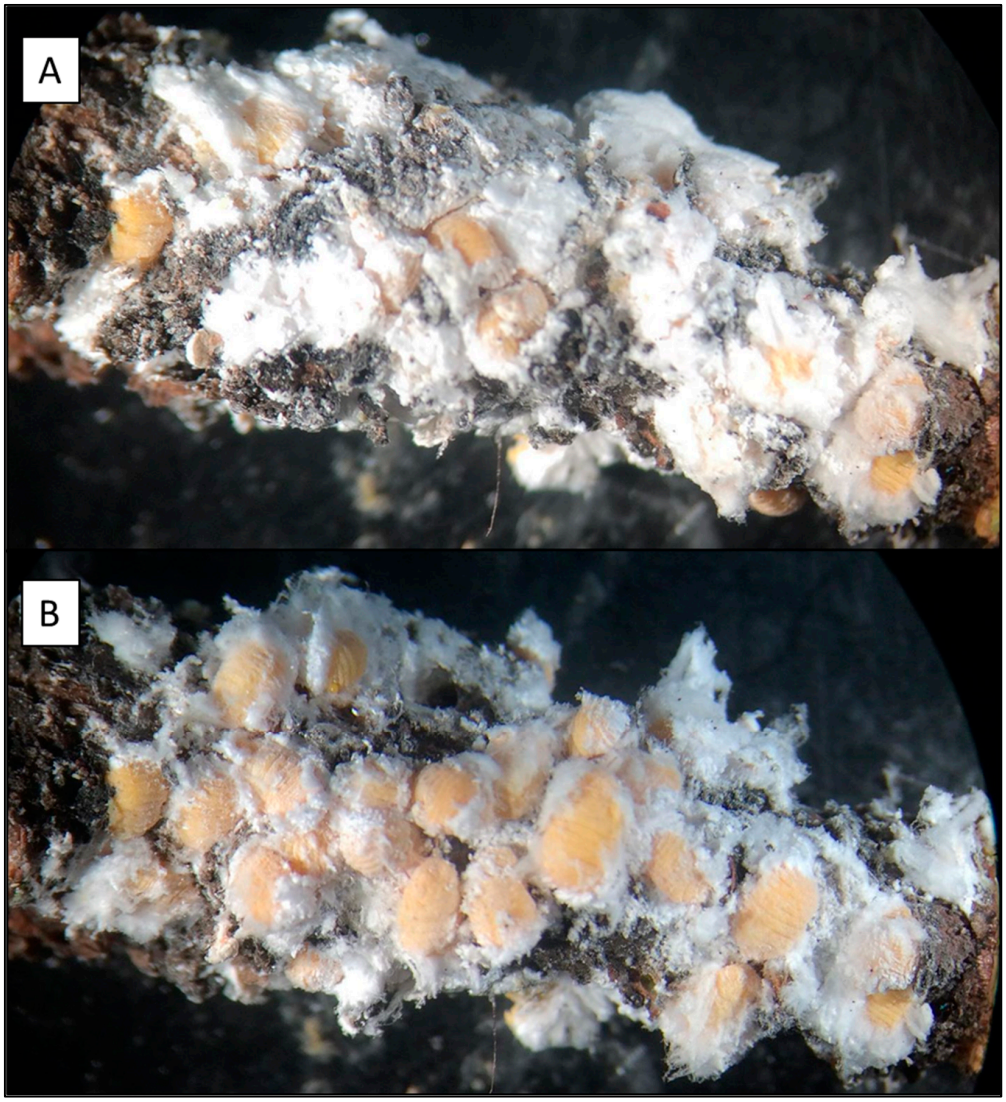

Figure 1. *Pinus radiata* twig, collected from CRP in March 2019, measuring 1.6 cm × 4.0 cm, and infested with 2nd instar stage *Marchalina hellenica.* Images show the same infested twig after excising (**A**) and after flocculent was removed (**B**). In view are 34 individual 2nd instar nymphs at a density of 0.60 GPS cm^{-2}.

Differences in fortnightly means of *M. hellenica* activity between site and generation groups were tested via ANOVA. Where ANOVA was used, Tukey's HSD was used for post-hoc comparison of differences among groups. Where data were determined to be

non-parametric via Levene's test of equal variances among groups, differences between site and generation groups were tested via KW. Group comparison via pairwise independent samples *t*-test where KW was used did not assume equal variances between groups. This process was done for GPS [cm^{-2}], HPI [cm^{-2}], and HV [µL]. HV [µL] was also compared across instar stages; however, here, individual insect honeydew volume is used, rather than fortnightly means. The natural log ($\ln(x)$) of HV [µL] was used instead of the untransformed HV [µL] values, as this enabled better clarification of differences between instar stages via KW and between generations and field sites via MWU.

Fortnightly climate means were used in regression analyses to predict GPS [cm^{-2}], HPI [%], HPI [cm^{-2}], and HV [µL] recorded fortnightly samples. HPI [cm^{-2}] and HV [µL] were $\ln(x)$ transformed prior to regression analysis, as this provided stronger climate models that were a better fit for the tested data. Climate variables included temperature (°C), RH (%), VPD (kPa), as recorded by exposed and bark fissure data loggers, and ambient temperature, cumulative rainfall (mm), and solar exposure (MJ m^{-2}). Statistics associated with these models may be found in the Appendix A Tables A9–A12. Indicators of data fit, correlation strength, and statistical clarity for regression models were used to draw comparisons between models: for instance, if the same climate variable would explain variation in insect activity when recorded from different data sources (i.e., bark fissure, exposed trunk, weather station). Models for predicting HPI [cm^{-2}] or HV [µL] were plotted for each of the climate variables sources from the data recorder that produced a statistically significant regression model with the strongest correlation strength. The relationship between HPI [cm^{-2}] or HV [µL] and solar exposure (MJ m^{-2}) was also plotted, although solar exposure (MJ m^{-2}) was only sourced from the Bureau of Meteorology. Approximate Nonlinear Durbin–Watson test was used to check for autocorrelation among HPI [cm^{-2}] or HV [µL] and climate variables [56,57].

Climate variables explaining a particular *M. hellenica* activity were included in multiple regression analysis with the goal of obtaining residual values for all climate variables included. Since climate variables were measured with differing units of measurement, standardised residual values were extracted. These standardised residual values were then included in a linear regression analysis to confirm that a given *M. hellenica* was responsive to the combined effect of the temperature (°C), RH (%), VPD (kPa), and solar exposure (MJ m^{-2}) records that most strongly correlated with *M. hellenica* activity. These standardised residual plots, with 95% confidence intervals of the mean, are visualized in Figures A1–A4.

3. Results

3.1. Seasonal Phenology

The onset and duration of seasonal feeding behaviour was visualized from January 2019 (Figure 2A), 2020 (Figure 2B), and up to October 2021 (Figure 2C). *Marchalina hellenica* 1st instar nymphs largely emerged from their eggs and ovisacs in late November (Figure 2A). First detection of instar stage emergences occurred progressively earlier with each year (Table A1), although not for the adult stage. In 2019, the first instars began moulting in February, but the first instars began moulting in late January and early February in 2020 and 2021. The persistence of the second instar appeared to shorten each year; it was present for 17 weeks in 2019, 16 weeks in 2020, and 12 weeks in 2021. The third instars were always initially detected in April. However, the time from the first time that the third instar was detected until 100% of insects sampled were third instars, was less in 2021 than earlier generations. The third instar stage was the longest persisting stage, lasting up to 7 months from April until October. Final ecdysis usually occurred around mid-September when the third instars moulted into adults. By mid-October 2019 and 2020, the third instars were absent.

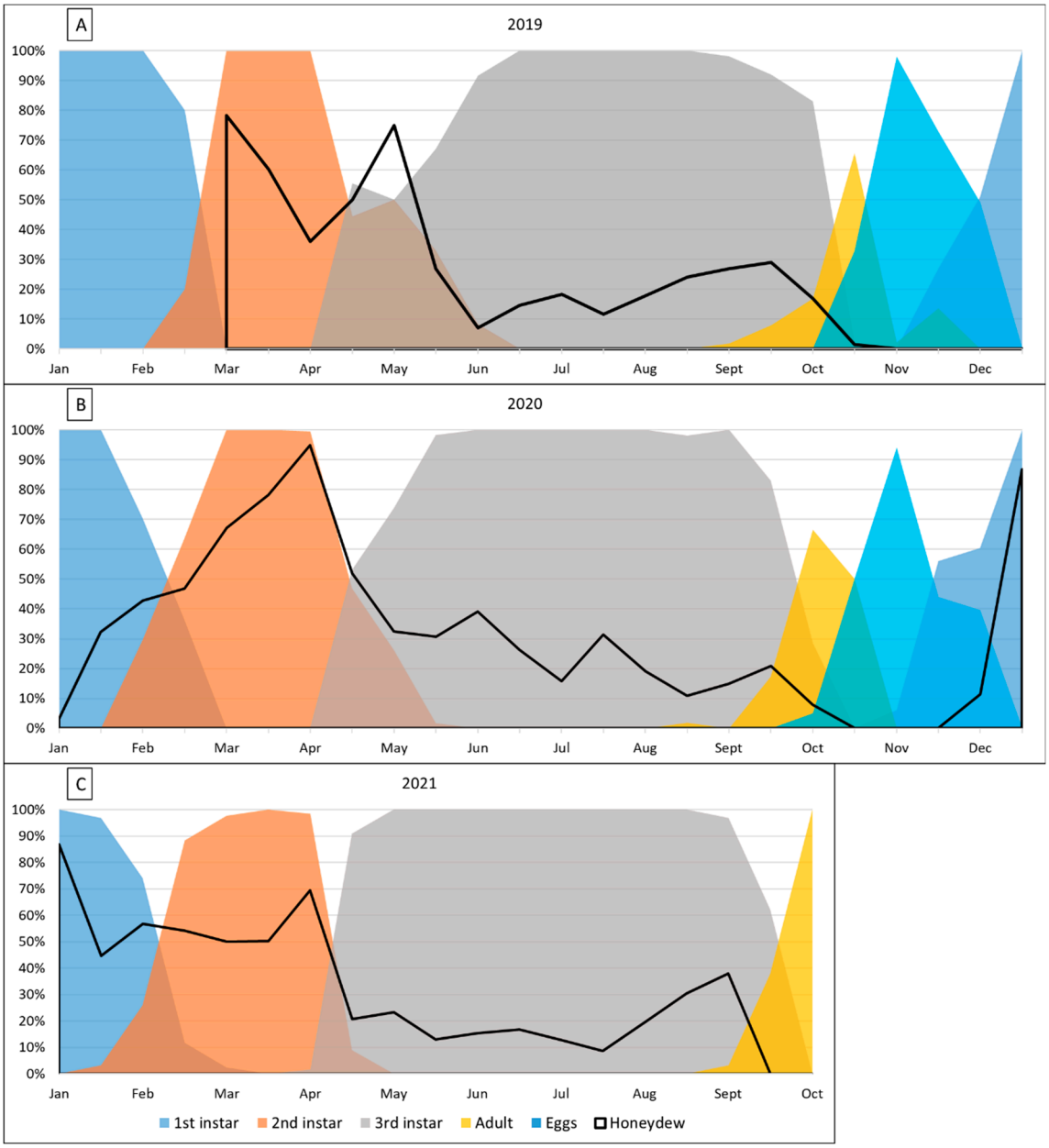

Figure 2. Phenology of *Marchalina hellenica* in Southeast Melbourne, showing the abundance of each life stages as a proportion of population in (**A**) 2019, (**B**) 2020, and (**C**) 2021, and the proportion of insects producing honeydew (black line).

Population progression also appeared to accelerate each year for adults. For populations sampled in mid-September, 8% of *M. hellenica* were adults in 2019, 17.24% in 2020, and 37.79% in 2021. Two adults were detected in mid-late August 2020, although none were found the next fortnight or in August of 2019 and 2021. Despite most adults being present during October, they may persist into November. Adults oviposit throughout late September and October, with eggs developing for approximately 4–6 weeks before emerging into first instar nymphs around late-November. Adult *M. hellenica* are semelparous organisms, meaning that they die after a single reproduction event. As a result, by the time the first instars emerge, the adults have almost entirely perished.

3.2. Feeding Activity

Data collection of honeydew producers in samples did not commence until 21 March 2019; hence, a sudden spike in honeydew availability was visualized in Figure 2A. Insects emerging in November 2019 were not detected as producing honeydew until early January 2020 (Figure 2B), compared to nymphs emerging November 2020, which commenced honeydew production in early December 2020 (Figure 2B). HPI [%] was significantly correlated with the proportion of second instar nymphs in a population (Pearson correlation, $r = 0.747$, $t = 7.368$, $p < 0.001$). As a percentage of the sampled population, the second instar stage was found to be most the likely to produce honeydew compared to all other life stages observed (Table A2). The exception to this was a two-week period from late December 2020 to early January 2021 when 86.80% of the first instar nymph population were producing honeydew (Figure 2C). HPI [%] did not exceed this percentage again in 2021, with 69.35% being the next highest in 2021, recorded from second instar nymphs in early April. As insects reach their second ecdysis, honeydew production decreased sharply in all generations. Third instar nymphs were much less likely to produce honeydew than second instar nymphs, with third instar HPI [%] never exceeding 50% during winter months. In all generations, there was a small but noticeable rise in HPI [%] from late August to early September of 2019 and 2021.

Analysis of *M. hellenica* density across 32 months revealed differences across temporally separated populations (Kruskal–Wallis test of independent samples (KW): $p = 0.023$, $F_{31,85} = 48.590$). Variability in mean density was visualized in Figure 3. Density was highest during November 2020, when *M. hellenica* first instar nymphs were emerging from eggs. Tukey's HSD provided evidence of density-related differences between specific temporal groups (Table A8), but since this test assumes a normal distribution and equal variances among groups, the outcome must be interpreted with caution. Most months could not be distinguished, with only November 2020 differing from a few months of 2020 and October 2019.

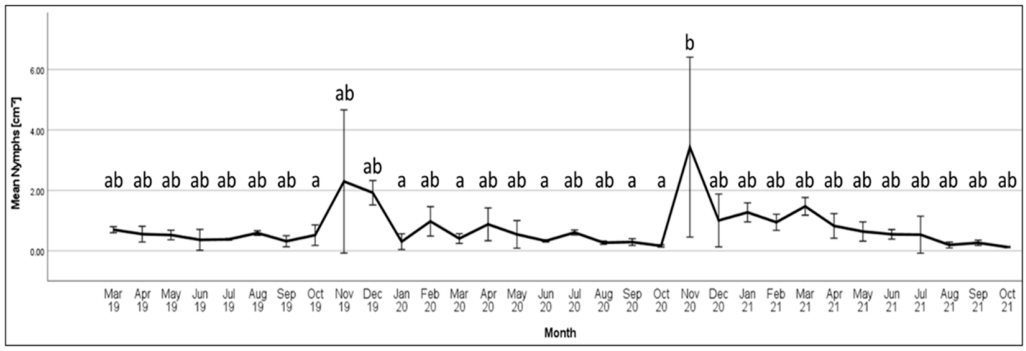

Figure 3. Seasonal mean density of *Marchalina hellenica* nymphs, combining samples from *Pinus radiata* at Dalton Reserve and Cardinia Reservoir Park across 32 months (±2 S.E). Significant differences are indicated by groups that do not share a letter (Tukey's HSD; $p < 0.05$). N ≥ 2 for March–July 2019, August 2020, and October 2021, N ≥ 4 for all other groups.

Ln(x) transformed volumes of honeydew produced per insect (HV [µL]) were found to increase with each instar stage (Kruskal–Wallis: $p < 0.001$, $F_{2,454} = 189.592$, Figure 4). Pairwise comparisons of each instar stage demonstrated significant differences between all group pairings, with HV [µL] production exhibiting an exponential increase as each successive instar stage is reached (Figure 4; Table A3). First and third instar stages demonstrated the most substantial difference in honeydew produced per insect (Table A4). First instars produced a mean volume of 0.019 µL, and the third instars produced a mean of 0.240 µL, which is approximately twelve-times more honeydew.

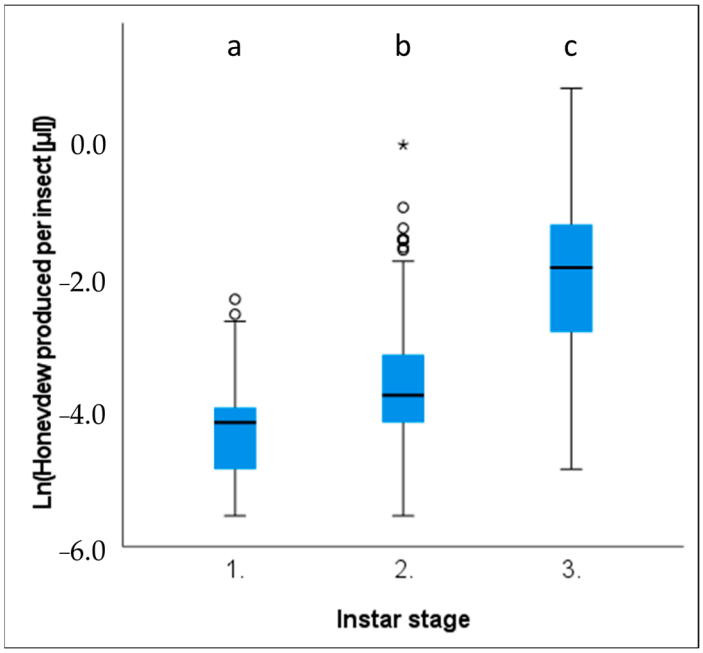

Figure 4. Box and whisker plot of honeydew volume (natural log transformed) produced per *Marchalina hellenica* nymph (ln (HV [µL])). Box and whisker boxes represent interquartile ranges, with the horizontal black line within the boxes indicating the group mean. Outliers are indicated by circles and asterisks. Significant differences between groups are indicated by different letters ($p < 0.05$).

Differences were identified between site and generation groups for GPS [cm^{-2}] (ANOVA: $p = 0.027$, $F_{5,106} = 2.647$), HPI [cm^{-2}] (KW: $p < 0.001$, $F_{5,93} = 25.822$), and HV [µL] (KW: $p < 0.001$, $F_{3,53} = 24.348$; Tables A5–A7). GPS [cm^{-2}] recorded at Dalton Reserve (DR) across 2020 was approximately 144% greater than the generation emerging at DR in 2019 (Tukey's HSD: $p = 0.039$, N = 47; Figure 5A). HPI [cm^{-2}] was approximately 242% greater at DR than Cardinia Reservoir Park (CRP) in 2019 (KW pairwise comparison: $p < 0.001$, $t = 25.822$, N = 93; Figure 5B). HV [µL] produced by *M. hellenica* was reduced for the 2020 generation compared to 2019 for both sites (Figure 5C). HV [µL] was approximately 55% lower in 2020 than 2019 at CRP (KW pairwise comparison: $p = 0.024$, $t = 2.876$, N = 26) and approximately 84% lower in 2020 than 2019 for DR (KW pairwise comparison: $p < 0.001$, $t = 3.927$, N = 27).

3.3. Insect Activity Response to Climate

Climate variables used to predict honeydew producer insects per cm^{-2} (HPI [cm^{-2}]) generally provided stronger and more statistically significant models compared to either GPS [cm^{-2}] or HPI [%] alone. This may be due to HPI [cm^{-2}] being a derivative accounting for both metrics. For this reason, only climate models specifically predicting HPI [cm^{-2}] and honeydew volume produced per insect (HV [µL]) are reported here. Only the strongest model for each climate variable was reported. Other model summaries of each *M. hellenica* activity variable and each climate record type are available in the Appendix A (Tables A9–A12). AND test did not reveal evidence of autocorrelation between climate variables and ln (HPI [cm^{-2}]), or climate variables and ln (HV [µL]), for statistically significant regression models (Tables A11 and A12).

Statistically significant trends were found clarifying that ln (HPI [cm^{-2}]) was at least weakly correlated with most climate variables (Table A11). As temperature increased, HPI [cm^{-2}] increased exponentially. Ambient temperature provided the strongest model correlation of this relationship (linear regression: $p < 0.001$, $F_{1,29} = 35.231$, $r^2 = 0.549$; Figure 6A) and indicated that increases in ambient temperature may explain approximately 53.3% of observed variation in ln (HPI [cm^{-2}]). Statistical evidence found that ln (HPI

[cm^{-2}]) was negatively related to exposed RH, which explained 27.9% of the variation observed in HPI [cm^{-2}] (linear regression: $p = 0.0013$, $F_{1,29} = 12.858$, $r^2 = 0.303$; Figure 6B). Natural log transformed HPI [cm^{-2}] was moderately correlated with exposed VPD (linear regression: $p < 0.001$, $F_{1,29} = 16.317$, $r^2 = 0.360$; Figure 6C), explaining approximately 33.8% of variation observed in HPI [cm^{-2}]. Higher solar exposure was found to be associated with exponential increases in HPI [cm^{-2}] (linear regression: $p = 0.015$, $F_{1,29} = 6.394$, $r^2 = 0.122$; Figure 6D). This was a weak correlation, with variation in solar exposure explaining approximately 10.3% of observed variation in HPI [cm^{-2}].

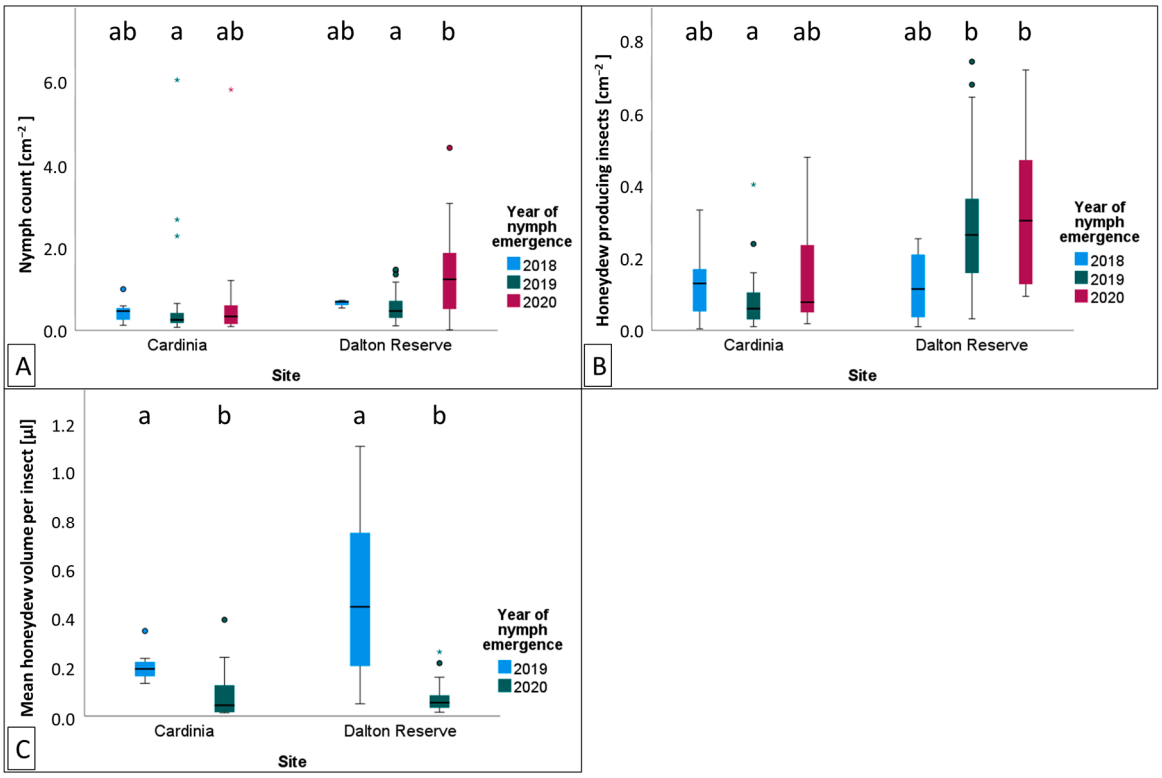

Figure 5. Box and whisker plots of *Marchalina hellenica* population activity at Cardinia or Dalton Reserve during the 2018, 2019 or 2020 emergent generations. *Marchalina hellenica* activity illustrated includes (**A**) nymph count per cm^2, (**B**) honeydew producing insects per cm^2, and (**C**) mean honeydew volume excreted per insect [µL]. Box and whisker boxes represent interquartile ranges, with the horizontal black line within the boxes indicating the group mean. Outliers are indicated by circles and asterisks. Significant differences between groups are indicated by different letters ($p < 0.05$).

Increases in exposed temperature records were moderately associated with exponential decreases in mean ln (HV [µL]) (linear regression: $p < 0.001$, $F_{1,27} = 40.061$, $r^2 = 0.597$; Figure 7A). Here, 58.2% of observed variation in HV [µL] could be explained by variation in exposed temperature. Regression modelling revealed that exponential increases in HV [µL] were moderately correlated with lower RH. This was only the case when the regression model utilised exposed RH records (linear regression: $p < 0.001$, $F_{1,27} = 15.360$, $r^2 = 0.363$; Figure 7B), which indicated that approximately 33.9% of variation observed in log transformed HV [µL] could be explained by exposed RH. Evidence was found to show HV [µL] was moderately correlated against exposed VPD (linear regression: $p < 0.001$, $F_{1,27} = 31.823$, $r^2 = 0.541$; Figure 7C), with an estimated 52.4% of variation observed in ln (HV [µL]) explained by exposed VPD. Very strong statistical significance was found in support of the observation that ln (HV [µL]) was negatively associated with mean solar exposure (linear regression: $p < 0.001$, $F_{1,27} = 18.976$, $r^2 = 0.380$; Figure 7D). This model had a moderately strong correlation, indicating that approximately 36% of observed variation in ln (HV [µL]) may be explained by variation in fortnightly mean solar exposure.

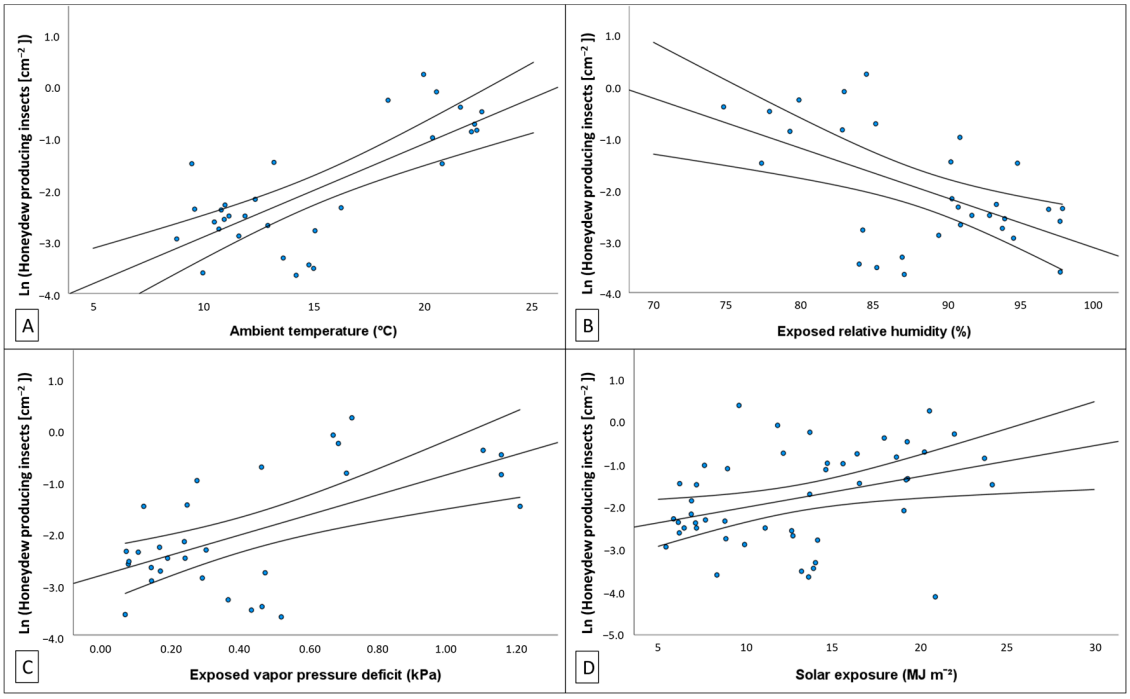

Figure 6. Relationship between natural log transformed fortnightly density of honeydew excreting nymphs (ln (HPI [cm^{-2}])) to (**A**) exposed temperature, (**B**) exposed relative humidity, (**C**) exposed vapor pressure deficit, and (**D**) solar exposure. Regression model is plotted as continuous black line, and curved lines indicate confidence intervals (95%) of the mean. Strong evidence was found that multiple climate variables correlate with, and explain, observed variation in ln (HPI [cm^{-2}]) (Table A11).

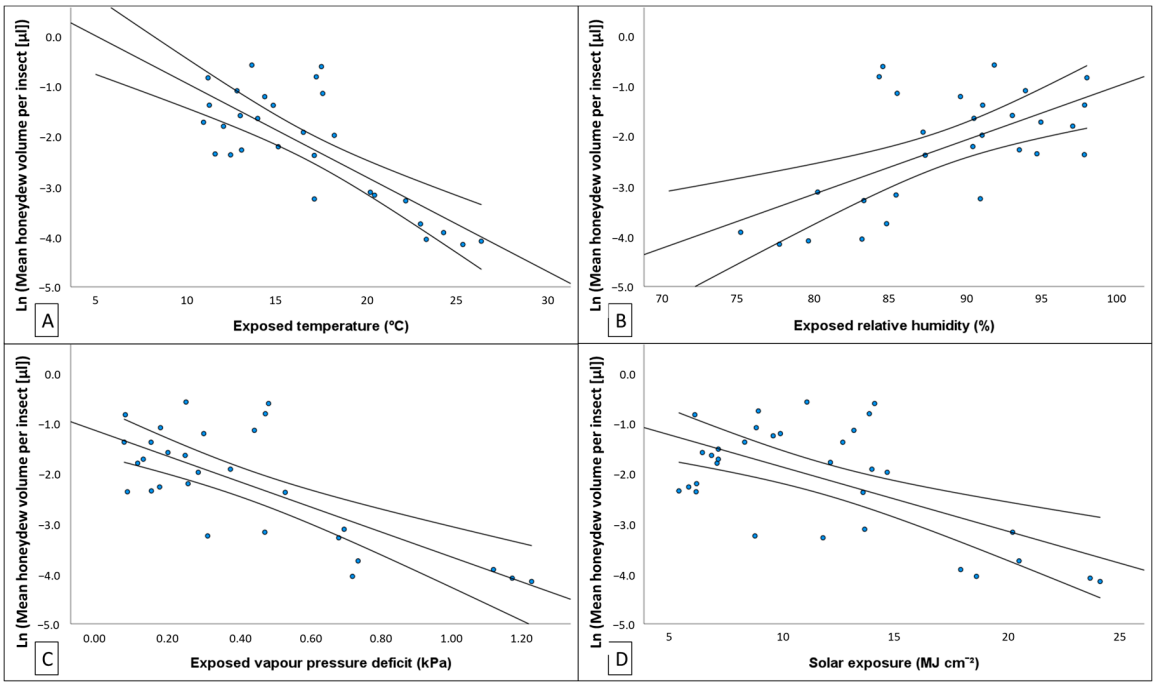

Figure 7. Relationship between natural log transformed fortnightly *Marchalina hellenica* honeydew excreted per insect (ln (HV [µL])) to (**A**) exposed temperature, (**B**) exposed relative humidity, (**C**) exposed vapor pressure deficit, and (**D**) solar exposure. Regression model is plotted as continuous black line, and curved lines indicate confidence intervals (95%) of the mean. Strong evidence was found that multiple climate variables correlate with, and explain, observed variation in ln (HV [µL]) (Table A12).

4. Discussion

Broad similarities were identified between Mediterranean and Australian *M. hellenica* populations in the timing of life stages in local seasons [31,53]. As expected, major developmental milestones typically exhibited a six-month delay between Mediterranean and Australian populations. In Australia, the occurrence of life stages between years of study was broadly similar, although the developmental stages showed progressive changes each year; for example, instar stages were detected earlier with successive generations. By contrast, in Greece [50,58], the timing of the occurrence of different instars varied between generations; however, initial detection of each life stage did not occur earlier or later with successive generations. Phenology and development can be delayed or accelerated by changes in climate, a trend observed in other scale insects [10], other Hemiptera [12], and other insect orders [7,53]. Given the relatively short time it has been present, Australian *M. hellenica* may still be adjusting to the effects of climate drivers on their activity. The current study was limited by the fragmented distribution of exotic *P. radiata* in Australia. Relating the seasonal phenology of *M. hellenica* in other climates to that in Australia would provide valuable attestation of the relationships identified here.

The densities of *M. hellenica* on Australian *P. radiata* were typically higher than Mediterranean conspecifics feeding on *Pinus halepensis* during seasonally equivalent months [51]; however, the proportion of honeydew producing insects did not reach proportions as high as those previously documented in Greece [50]. We found evidence that variation in the density of honeydew producing insects and the quantity of honeydew produced could be explained by changes in temperature, humidity, vapour pressure in the atmosphere, and solar exposure. Depending on where climate was recorded (i.e., weather station, exposed tree trunk or bark fissure), the degree of association *M. hellenica* demonstrated with climate variables varied greatly in this study. The insect's flocculent and preference for crevices and non-sun facing aspects [59] realises a microclimate distinct from broader forest conditions. Microhabitat climate was found to provide weaker predictions of insect activity, as it directly records the climate experienced by sheltered ectothermic *M. hellenica* [37], rather than the experience of the host. With regards to this study, the climate, as experienced by the host, most often provided the best predictive models.

In Australia, variation in the density of *M. hellenica* nymphs and proportion of honeydew producing insects (HPI [%]) were associated with warmer and drier conditions. HPI [%] in Australia was often higher over winter than reported in Greece [50]; however, unlike honeydew availability in Greece, there were no instances where 100% of *M. hellenica* sampled in Australia were excreting honeydew. Broadly, Australian HPI [%] followed similar seasonal patterns to Mediterranean observations, including an increase in honeydew availability following overwintering. Since the phenological study from Greece occurred from 2001 to 2003, it is unclear whether the difference in findings between the current study and previous observations are attributable to underlying geographic differences, inherent generational variation, or host species. The insect density recorded in the current study, from 2019–2020, was only separated by six months from insect densities recorded from Greek conspecifics in 2018–2019 [51]. However, the density of Australian *M. hellenica* was generally higher than the density of the concurrent Greek conspecifics. Insect density, HPI [%], and HPI [cm^{-2}] showed a positive relationship with temperature and atmospheric vapour pressure deficit (VPD) and negative association with rainfall and RH. The volume of honeydew produced per insect had the opposite associations with these same climate variables. These relationships with environmental conditions may explain why *M. hellenica* in Australia achieved greater densities than Mediterranean populations. *Marchalina hellenica* in Australia may occupy a more solar exposed, warmer, and drier climate than Mediterranean conspecifics, which are conducive to *Pinus* growth [60,61] and, by association, tree quality as a host for herbivores [62,63]. Unlike previous studies showing microclimate better reflects insect ontogeny, compared to macroclimate records [37], climate conditions within the microhabitat of settled *M. hellenica* nymphs in this study were usually not the best indicator of changes in insect activity. This may be due to strong climate effects on

the host's activity [64,65], and therefore, the availability of resources for *M. hellenica*. The influence of host quality on phloem-feeder activity may therefore be amplified because settled *M. hellenica* are sheltered from direct effects of forest climate condition and depend on climate-driven phloem enrichment [66]. Indeed, phloem-feeder honeydew production and density can fluctuate in association with daily cycles of phloem enrichment [13] and chemical defensive responses [51].

The highest recorded density for Australian *M. hellenica* in this study was over 5 *M. hellenica* per cm^2, compared to the highest density recorded in Greece of approximately 1.4 *M. hellenica* per cm^2 [51]. Both of these maximum density records coincided with first instar emergence, and at other times, Greek *M. hellenica* densities were close to zero for most months, and almost always less than 0.25 *M. hellenica* per cm^2. By contrast, Australian density presented here was 0.5 per cm^2 or higher across most months. One explanation for elevated *M. hellenica* density in Australia compared to Greece may be that the insect has escaped its natural enemies. The notable enemy is the predatory fly, *Neoleucopis kartliana*, a monophagous predator and prospective biocontrol agent [53,67]. *Neoleucopis kartliana* is recorded as being the most effective and widely distributed predator of *M. hellenica* in Turkey [32]. With *N. kartliana* absent, *M. hellenica* populations in Australia may proliferate with relatively little impact from natural enemies [68–70]. If *N. kartliana* is deemed suitable for introduction into Australia as a classical biocontrol agent, inoculative mass-releases of this fly may be guided by the seasonal patterns of Australian *M. hellenica* documented here. For example, the effectiveness of biological control agents can be heavily dependent on the presence of particular life stages, not just any individual, from a given target species [71]. This may be critical to any future release of *N. kartliana*, as the timing of its phenology matches the seasonal phenology of *M. hellenica* [53].

Host species is also likely important for *M. hellenica* growth and survival. In the Mediterranean, *Pinus halepensis* is the primary host for *M. hellenica*, a tree that shares a long history of hosting *M. hellenica*, which provide honeydew as an alternative to floral nectar for apicultural purposes [17]. This relationship dates back to the late Roman and early Byzantine Empires along the east coast of the Mediterranean Sea [19,29,72]. A long co-evolutionary history may also be implied by *P. halepensis* possessing targeted defence responses that coincide with seasonal nymph emergence [51,73]. With *M. hellenica* recorded as acquiring the novel host in 2014 [16], *P. radiata* in Australia may be lacking specific defence adaptations that have evolved in *P. halepensis*. Even if *P. radiata* has a similar seasonal-specific defence, the shifting phenology of *M. hellenica* in Australia may allow the insect to escape a temporally restricted defence by emerging earlier. A similar process is documented in other insects (e.g., aphids, bark beetles, Heteroptera), notably involving interactive effects with regional climate [74–76] or broadscale climate change [5,42,77].

This study's findings are similar to previous investigations linking climate to changes in both plant and herbivore activity [76,78–81]. Climate effects may therefore affect the quality of *M. hellenica* as a host for predatory insects, as has been observed in parasitic/predatory Diptera [82,83]. *Marchalina hellenica* occurs in areas of similar climate conditions to its endemic Greek distribution [67] and is largely dependent on *P. radiata* phloem feeding—the quality of which is influenced by climate conditions [74,84]. For example, VPD is known to be a driver of daily cycles of transpiration and photosynthesis in *Pinus* [40,85,86] and responses to novel climate conditions may alter phloem quality for herbivores. In *Pinus*, these responses are a result of tight regulation of stomatal pore closure and, therefore, strict responses in transpiration, photosynthetic activity, or enrichment of phloem elements [87–89]. With such rapid responses to environmental changes, *M. hellenica*, by expropriating carbohydrates, amino acids, and other macromolecules [24], may illicit these strict responses [90] and potentially exacerbate stressful climate effects on the host tree. As global climate conditions deviate from previous means, this insect may experience changes in phenological timing and feeding activity [5,7,91]. Investigation of how *M. hellenica* life cycle and feeding activity may respond to changes to environmental conditions in its endemic geographic

range or on native hosts would provide valuable comparisons with the relationships identified in Melbourne populations.

Author Contributions: Conceptualization, D.D.J., J.P.C., D.I.S. and M.J.S.; data curation, D.D.J.; formal analysis, D.D.J. and M.J.S.; funding acquisition, J.P.C. and M.J.S.; investigation, D.D.J. and M.J.S.; methodology, D.D.J., J.P.C., D.I.S. and M.J.S.; project administration, M.J.S.; resources, D.D.J., J.P.C., D.I.S. and M.J.S.; visualization, D.D.J., J.P.C., D.I.S. and M.J.S.; supervision, J.P.C., D.I.S. and M.J.S.; writing—original draft, D.D.J., J.P.C. and D.I.S.; writing—review and editing, D.D.J., J.P.C., D.I.S. and M.J.S. All authors have read and agreed to the published version of the manuscript.

Funding: This research is part of a PhD project funded by scholarship and operating funds provided by Forest & Wood Products Australia Limited (VNC472-1819). Additional funding was provided by La Trobe University to M.J.S for the supervision of D.D.J.

Data Availability Statement: The data presented in this study are available on request from the corresponding author.

Acknowledgments: Thank you to Breanna Butera, Hannah Young, Loretta Gibilisco, and Sam Heywood for support and during initial field site assessments, collections, and sample inspections. Thank you to James Martin who assisted with field the bulk of field work during Melbourne's COVID-19 lockdown. Thank you to Greg Lefoe and Umar Lubanga for providing feedback on late-stage drafts. Thanks to Angus Carnegie for inviting M.J.S. to propose this PhD project.

Conflicts of Interest: The authors declare no conflict of interest. The funders had no role in the design of the study; in the collection, analyses, or interpretation of data; in the writing of the manuscript; or in the decision to publish the results.

Appendix A

Table A1. Summary statistics of first detections of notable life history milestones and feeding activity across *Marchalina hellenica* instars of a given generation. ± represents one standard deviation.

Generation	Nymph Emergence	1st Ecdysis	2nd Ecdysis	Final Ecdysis	Mean HPI (%)	Max HPI (%)
2018–2019	22 November 2018	11 February 2019	26 April 2019	9 September 2019	30.82 ± 24.66	78.33
2019–2020	18 November 2019	5 February 2020	12 April 2020	28 August 2020	32.82 ± 25.90	95.84
2020–2021	12 November 2019	29 January 2021	8 April 2021	10 September 2021	37.13 ± 22.18	86.80

Table A2. Maximum potential temporal range of each *Marchalina hellenica* instar stage and the mean percent of settled insects (SI) and honeydew producing insects (HPI) across phenological records.

Instar Stage	Max Recorded Temporal Range	SI (%)	HPI (%)
1st	12 November–25 February	90.65	33.58
2nd	29 January–7 June	86.88	54.40
3rd	12 April–23 October	73.24	21.81

Table A3. Pairwise comparison (equal variances not assumed) to identify if honeydew volume produced by individual *Marchalina hellenica* differed between instar stages. All pairs differences are statistically significant ($p < 0.05$).

Instar Stage	Instar Stage	Mean Diff. (µL)	Std. Error
1	2	0.585	0.119
	3	2.234	0.124
2	1	0.585	0.119
	3	1.658	0.127
3	1	2.243	0.124
	2	1.658	0.127

Table A4. Summary of *Marchalina hellenica* honeydew volume produced by instar stage. Sample sizes vary due to differences in honeydew production rates and temporal distribution.

Instar Stage	Max Honeydew (µL)	Mean Honeydew (µL)	Std. Deviation (µL)	N
1st	0.0977	0.019	0.018	98
2nd	0.9688	0.051	0.094	166
3rd	2.2500	0.240	0.342	190

Table A5. Summary of Tukey's HSD post-hoc testing differences in the density of *Marchalina hellenica* between site and generation groups.

Group 1	Group 2	*p*	Mean Difference (cm^{-2})	Standard Error of the Mean
Cardinia 2018	Cardinia 2019	0.998	−0.158	0.349
	Cardinia 2020	0.995	−0.191	0.367
	Dalton Reserve 2018	0.999	−0.211	0.566
	Dalton Reserve 2019	0.999	−0.137	0.356
	Dalton Reserve 2020	0.092	−0.977	0.367
Cardinia 2019	Cardinia 2020	0.999	−0.033	0.272
	Dalton Reserve 2018	0.999	−0.053	0.509
	Dalton Reserve 2019	0.999	0.021	0.256
	Dalton Reserve 2020	0.037	−0.819	0.272
Cardinia 2020	Dalton Reserve 2018	0.999	−0.019	0.522
	Dalton Reserve 2019	0.999	0.054	0.281
	Dalton Reserve 2020	0.092	−0.786	0.295
Dalton Reserve 2018	Dalton Reserve 2019	0.999	0.073	0.514
	Dalton Reserve 2020	0.684	−0.767	0.523
Dalton Reserve 2019	Dalton Reserve 2020	0.039	−0.84	0.281

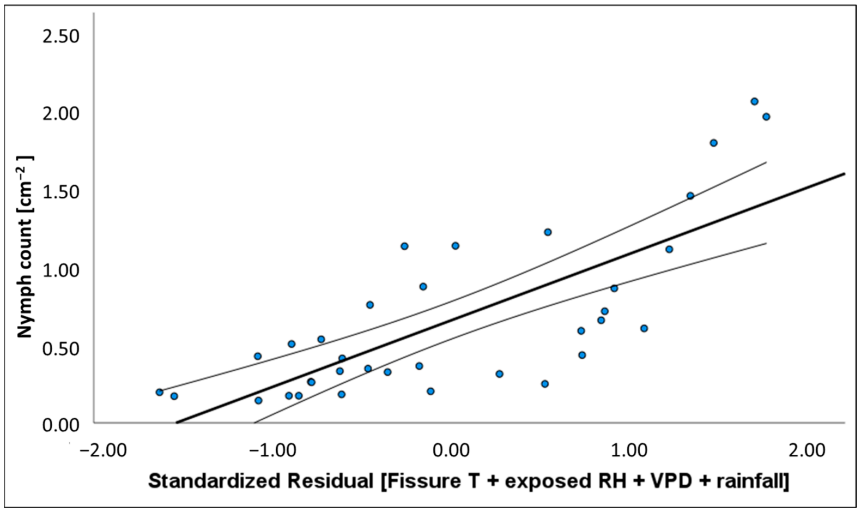

Figure A1. Scatterplot of *Marchalina hellenica* nymph density (cm^{-2}) plotted over standardised residual of best climate predictor variables. Regression model is plotted as continuous black line, and curved black lines indicate 95% confidence intervals of the mean. Climate variables were selected if they provided the strongest model identified for a given climate variable. Summary: $p < 0.001$, $F_{1,33} = 44.439$, $r^2 = 0.574$; model equation: $Y = 0.427x + 0.656$.

Table A6. Summary of Kruskal-Wallis pairwise comparison testing for differences in the density of honeydew producing nymphs (cm^{-2}) between site and generation groups.

Group 1	Group 2	*p*	Mean Difference (cm^{-2})	Standard Error of the Mean	Standardized *t* Statistic
Cardinia 2018	Cardinia 2019	0.999	0.046	10.753	0.914
	Cardinia 2020	0.999	−0.024	10.922	0.242
	Dalton Reserve 2018	0.999	0.012	16.219	0.098
	Dalton Reserve 2019	0.573	−0.167	10.753	2.072
	Dalton Reserve 2020	0.238	−0.192	10.922	2.413
Cardinia 2019	Cardinia 2020	0.999	−0.071	8.546	1.46
	Dalton Reserve 2018	0.999	−0.034	14.724	0.56
	Dalton Reserve 2019	0.002	−0.213	8.329	3.856
	Dalton Reserve 2020	<0.001	−0.238	8.546	4.234
Cardinia 2020	Dalton Reserve 2018	0.999	0.036	14.848	0.284
	Dalton Reserve 2019	0.323	−0.142	8.546	2.299
	Dalton Reserve 2020	0.102	−0.167	8.757	2.708
Dalton Reserve 2018	Dalton Reserve 2019	0.999	−0.179	14.724	1.621
	Dalton Reserve 2020	0.899	−0.204	14.848	1.881
Dalton Reserve 2019	Dalton Reserve 2020	0.999	−0.025	8.546	0.476

Table A7. Summary of Kruskal-Wallis pairwise comparison testing for differences in the mean volume of honeydew produced per nymph (μL), between site and generation groups.

Group 1	Group 2	*p*	Mean Difference (μL)	Standard Error of the Mean	Standardized *t* Statistic
Cardinia 2019	Cardinia 2020	0.024	0.112	6.366	2.876
	Dalton Reserve 2019	0.999	−0.28	7.095	0.941
	Dalton Reserve 2020	0.036	0.125	6.366	2.747
Cardinia 2020	Dalton Reserve 2019	<0.001	−0.392	6.154	4.06
	Dalton Reserve 2020	0.999	0.013	5.297	0.155
Dalton Reserve 2019	Dalton Reserve 2020	<0.001	0.405	6.154	3.927

Table A8. Summary of Tukey's Honestly Significant Differences post-hoc analysis of seasonal density collected across 32-months. Only month pairs that demonstrated significant differences in *Marchalina hellenica* density (GPS cm^{-2}) are shown ($p < 0.05$). Differences were only detected when comparing November 2020, thus all comparisons shown are comparisons with insect density recorded in November 2020.

Month Compared	Significance Level (*p*)	Mean Difference (GPS [cm^{-2}])	Std. Error of Mean
October 2019	0.029	2.915	0.697
January 2020	0.012	3.130	0.697
March 2020	0.041	3.027	0.745
June 2020	0.031	3.106	0.745
September 2020	0.011	3.143	0.697
October 2020	0.006	3.271	0.697

Table A9. Summary of climate regression models predicting *Marchalina hellenica* density. Climate records used in models represent the fortnightly mean value of daily maximum, except rainfall; recorded cumulatively in millimetres. N = 34 for each regression analyses.

	Predictor	**Model Equation Y =**	**F**	***p***	r^2	**Adj.** r^2
Ambient	Temperature [°C]	$0.060x - 0.261$	12.411	<0.001	0.273	0.251
	Solar Exposure [MJ m^{-2}]	$1.418x + 13.982$	1.366	0.251	0.040	0.011
Exposed	Temperature [°C]	$0.057x - 0.340$	12.641	<0.001	0.277	0.255
	RH [%]	$-0.051x + 5.142$	18.318	<0.001	0.357	0.337
	VPD [kPa]	$0.698x + 0.324$	10.774	0.002	0.246	0.223
Fissure	Temperature [°C]	$0.870x - 0.687$	17.164	<0.001	0.342	0.322
	RH [%]	$-0.041x + 4.396$	4.883	0.034	0.129	0.103
	VPD [kPa]	$1.591x + 0.235$	9.456	0.004	0.223	0.199
Melb. Water	Rainfall [mm]	$-0.010x + 0.871$	3.101	0.088	0.086	0.058

Table A10. Summary of climate regression models predicting the percentage of honeydew producing *Marchalina hellenica*. Climate records used in models represent the fortnightly mean value of daily maximum, except rainfall; recorded cumulatively in millimetres. N = 30 for each regression analyses.

	Predictor	**Model Equation Y =**	**F**	***p***	r^2	**Adj.** r^2
Ambient	Temperature [°C]	$0.028x - 0.118$	19.177	<0.001	0.398	0.377
	Solar Exposure [MJ m^{-2}]	$0.018x + 0.079$	8.414	0.007	0.225	0.198
Exposed	Temperature [°C]	$0.022x - 0.077$	10.617	0.003	0.298	0.243
	RH [%]	$-0.012x + 1.355$	4.706	0.038	0.140	0.110
	VPD [kPa]	$0.215x + 0.208$	4.293	0.047	0.129	0.099
Fissure	Temperature [°C]	$0.031x - 0.166$	11.296	0.002	0.280	0.256
	RH [%]	$-0.011x + 1.305$	1.951	0.173	0.063	0.031
	VPD [kPa]	$0.42x + 0.195$	2.976	0.095	0.093	0.062
Melb. Water	Rainfall [mm]	$0.001x + 0.289$	0.048	0.828	0.002	0.033

Table A11. Summary of climate regression models predicting log (mean HPI density [no cm^{-2}]). Climate records used in models represent the fortnightly mean value of daily maximum, except rainfall; recorded cumulatively in millimetres. N = 30 for each regression analysis. The absence of autocorrelation of the data is rejected if the Approximate Nonlinear Durbin-Watson (AND) statistic is less than 0.622 or greater than 2.041.

	Predictor	**Model Equation Y =**	**F**	***p***	r^2	***Adj.*** r^2	**AND**
Ambient	Temperature [°C]	$0.180x - 4.711$	35.231	<0.001	0.549	0.533	1.136
	Solar Exposure [MJ m^{-2}]	$0.106x - 3.315$	10.122	0.003	0.259	0.233	0.633
Exposed	Temperature [°C]	$0.161x - 4.746$	25.174	<0.001	0.465	0.446	0.993
	RH [%]	$-0.097x + 6.536$	12.858	0.0013	0.303	0.279	0.754
	VPD [kPa]	$1.98x - 2.858$	16.317	<0.001	0.360	0.338	0.981
Fissure	Temperature [°C]	$0.23x - 5.483$	30.523	<0.001	0.513	0.496	1.194
	RH [%]	$-0.082x + 5.466$	3.772	0.062	0.115	0.085	0.509
	VPD [kPa]	$3.847x - 2.975$	10.081	0.004	0.258	0.232	0.734
Melb. Water	Rainfall [mm]	$-0.014x - 1.727$	0.939	0.340	0.031	0.002	0.534

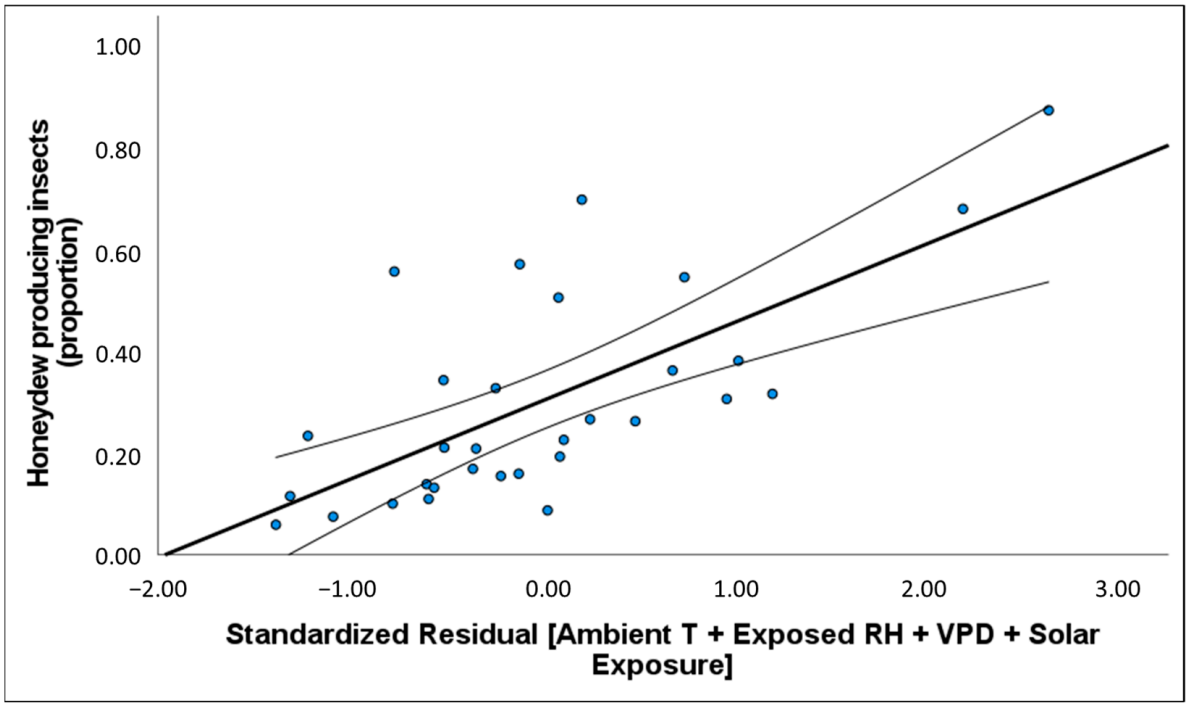

Figure A2. Scatterplot of the percentage of honeydew producing *Marchalina hellenica* plotted over standardised residual of best climate predictor variables with linear regression model plotted as curved black line. Curved black lines indicate 95% C. I. of the mean. Climate variables were selected if they provided the strongest model identified for a given climate variable. Summary: $p < 0.001$, $F_{1,29} = 26.031$, $r^2 = 0.473$; model equation: $Y = 0.153x + 0.3$.

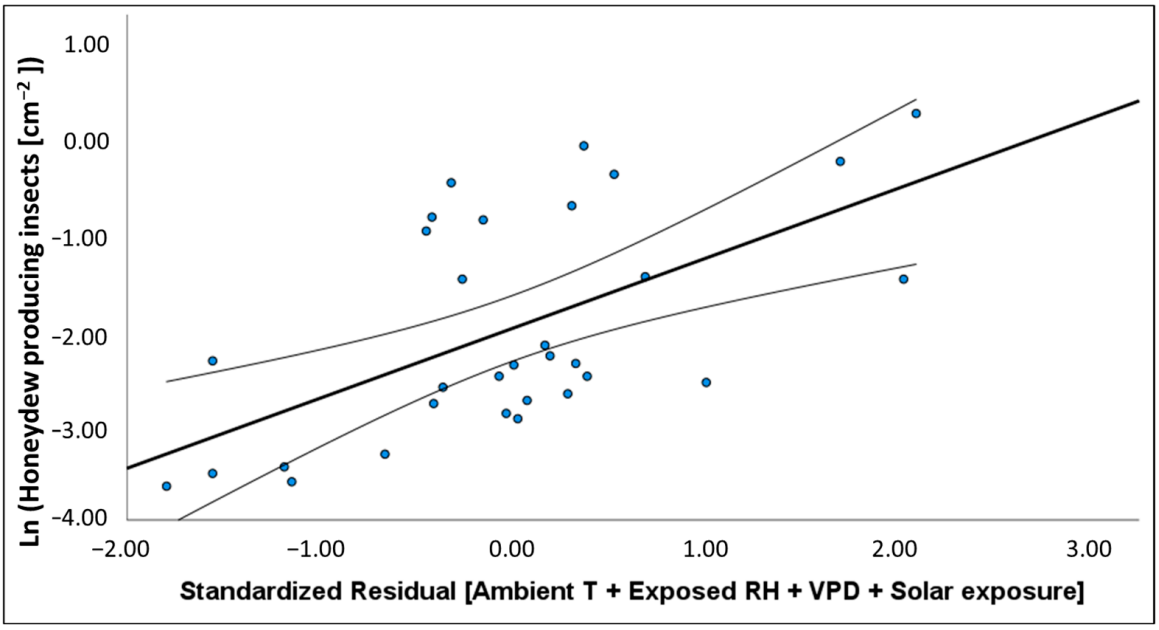

Figure A3. Scatterplot of log transformed density of honeydew producing *Marchalina hellenica* (cm^{-2}) plotted over standardised residual of best climate predictor variables with exponential regression model plotted as curved black line. Curved black lines indicate 95% confidence interval of the mean. Climate variables were plotted if they provided the strongest model identified for equivalent climate variable. Summary: $p < 0.001$, $F_{1,29} = 15.814$, $r^2 = 0.353$; model equation: $Y = 0.727 \times \log(x) - 2.008$.

Table A12. Summary of climate regression models predicting log (mean volume of honeydew produced per *M. hellenica* sampled), with zeros removed. Climate records used in models represent the fortnightly mean value of daily maximum, except rainfall; recorded cumulatively in millimetres. N = 28. The absence of autocorrelation of the data is rejected if the Approximate Nonlinear Durbin-Watson (AND) statistic is less than 0.566 or greater than 2.098.

	Predictor	Model Equation Y =	F	p	r^2	Adj. r^2	AND
Ambient	Temperature [°C]	$-0.183x + 0.511$	34.286	<0.001	−0.559	0.543	1.041
	Solar Exposure [MJ m^{-2}]	$-0.122x - 0.729$	15.591	<0.001	0.366	0.343	0.750
Exposed	Temperature [°C]	$-0.187x + 0.928$	40.061	<0.001	0.597	0.582	0.878
	RH [%]	$0.106x - 11.643$	15.360	<0.001	0.363	0.339	0.781
	VPD [kPa]	$-2.543x - 1.157$	31.823	<0.001	0.541	0.524	0.944
Fissure	Temperature [°C]	$-0.242x + 1.427$	30.820	<0.001	0.533	0.516	0.903
	RH [%]	$0.041x - 5.970$	0.858	0.362	0.031	0.005	0.498
	VPD [kPa]	$-3.768x - 1.278$	8.337	0.008	0.236	0.208	0.580
Melb. Water	Rainfall [mm]	$-0.007x - 2.073$	0.210	0.650	0.008	0.029	0.507

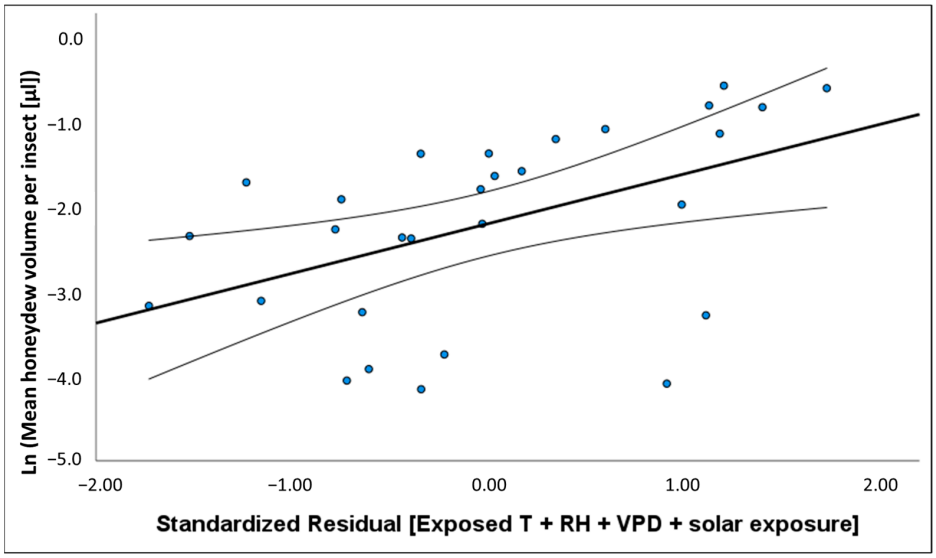

Figure A4. Scatterplot of log transformed mean honeydew volume excreted by *Marchalina hellenica* (µL) plotted over standardised residual of best climate predictor variables with exponential regression model plotted as curved black line. Curved black lines indicate 95% confidence interval of the mean. Climate variables were plotted if they provided the strongest model identified for equivalent climate variable. Summary: $p = 0.008$, $F_{1,27} = 8.196$, $r^2 = 0.233$; model equation: $Y = 0.583 \times \log(x) - 2.215$.

References

1. Holway, D.A.; Lach, L.; Suarez, A.V.; Tsutsui, N.D.; Case, T.J. The causes and consequences of ant invasions. *Annu. Rev. Ecol. Syst.* **2002**, *33*, 181–233. [CrossRef]
2. Xu, H.; Ding, H.; Li, M.; Qiang, S.; Zongguo, H.; Han, Z.; Huang, Z.; Sun, H.; Zhengmin, H.; Wu, H.; et al. The distribution and economic losses of alien species invasion to China. *Biol. Invasions* **2006**, *8*, 1495–1500. [CrossRef]
3. Kenis, M.; Auger-Rozenberg, M.-A.; Roques, A.; Timms, L.; Péré, C.; Cock, M.; Settele, J.; Augustin, S.; Lopez-Vaamonde, C. Ecological effects of invasive alien insects. *Biol. Invasions* **2009**, *11*, 21–45. [CrossRef]
4. Lester, P.J.; Beggs, J.R.; Brown, R.L.; Edwards, E.D.; Groenteman, R.; Toft, R.J.; Twidle, A.M.; Ward, D. The outlook for control of New Zealand's most abundant, widespread and damaging invertebrate pests: Social wasps. *N. Z. Sci. Rev.* **2013**, *70*, 54–60.
5. Yang, L.H.; Rudolf, V.H.W. Phenology, ontogeny and the effects of climate change on the timing of species interactions. *Ecol. Lett.* **2010**, *13*, 1–10. [CrossRef]
6. Lowry, E.; Rollinson, E.; Laybourn, A.J.; Scott, T.E.; Aiello-Lammens, M.; Gray, S.; Mickley, J.; Gurevitch, J. Biological invasions: A field synopsis, systematic review, and database of the literature. *Ecol. Evol.* **2013**, *3*, 182–196. [CrossRef]

7. Van Asch, M.; van Tienderen, P.G.; Halleman, L.J.M.; Visser, M.E. Predicting adaptation of phenology in response to climage change, an insect herbivore example. *Glob. Chang. Biol.* **2007**, *13*, 1596–1604. [CrossRef]
8. Lubanga, U.K.; Taylor, G.S.; Steinbauer, M.J. Developmental biology and seasonal phenology of *Aacanthocnema dobsoni* (Hemiptera: Triozidae) and the influence of climate-mediated changes in body size on vibrational signals. *Austral Entomol.* **2021**, *60*, 234–243. [CrossRef]
9. Banfield-Zanin, J.A.; Leather, S.R. Season and drought stress mediate growth and weight of the green spruce aphid on Sitka spruce. *Agric. For. Entomol.* **2015**, *17*, 48–56. [CrossRef]
10. Magalhães, T.A.; Oliveira, D.S.; Isaias, R.M.S. Population dynamics of the gall inducer *Eriogallococcus isaias* (Hemiptera: Coccoidea: Eriococcidae) on *Pseudobombax grandiflorum* (Malvaceae). *J. Nat. Hist.* **2015**, *49*, 789–801. [CrossRef]
11. Calatayud, P.A.; Tertuliano, M.; Rü, B. Seasonal changes in secondary compounds in the phloem sap of cassava in relation to plant genotype and infestation by *Phenacoccus manihoti* (Homoptera: Pseudococcidae). *Bull. Entomol. Res.* **1994**, *84*, 453–459. [CrossRef]
12. Nielsen, A.L.; Hamilton, G.C.; Shearer, P.W. Seasonal phenology and monitoring of the non-native *Halyomorpha halys* (Hemiptera: Pentatomidae) in soybean. *Comm. Ecosys. Ecol.* **2011**, *40*, 231–238. [CrossRef]
13. Taylor, S.H.; Parker, W.E.; Douglas, A.E. Patterns in aphid honeydew production parallel diurnal shifts in phloem sap composition. *Entomol. Exp. Appl.* **2011**, *142*, 121–129. [CrossRef]
14. Nahrung, H.F.; Loch, A.D.; Matsuki, M. Invasive insects in Mediterranean forest systems: Australia. In *Insects and Diseases of Mediterranean Forest Systems*; Paine, T.D., Lieutier, F., Eds.; Springer: Cham, Switzerland, 2016; pp. 475–498.
15. Nahrung, H.F.; Carnegie, A.J. Boarder interceptions of forest insects established in Australia: Intercepted invaders travel early and often. *NeoBiota* **2021**, *64*, 69–86. [CrossRef]
16. Agriculture Victoria: Pests, Insects and Other Invertebrates: Giant Pine Scale. Available online: https://agriculture.vic.gov.au/biosecurity/pest-insects-and-mites/priority-pest-insects-and-mites/giant-pine-scale (accessed on 26 October 2018).
17. Avtzis, N. *Marchalina hellenica* (*Monophlebus hellenicus*) Genn. Greece's most important honey-bearing insect. *For. Res.* **1985**, *6*, 51–64.
18. Üglentürk, S.; Özdemir, I.; Kozár, F.; Kaydan, M.B.; Dostbil, Ö.; Sarıbaşak, H.; Civelek, H.S. Honeydew producing insect species in forest areas in Western Turkey. *Turk. Bull. Entomol.* **2013**, *3*, 125–133.
19. Mendel, Z.; Manuela, B.; Battisti, A. Invasive sap-sucker insects in the Mediterranean Basin. In *Insects and Diseases of Mediterranean Forest Systems*; Paine, T.D., Lieutier, F., Eds.; Springer: Cham, Switzerland, 2016; pp. 261–291.
20. ABARES, Australian Bureau of Agricultural and Resource Economics and Sciences: Australian Plantation Statistics 2022 Update. Available online: https://daff.ent.sirsidynix.net.au/client/en_AU/ABARES/search/detailnonmodal/ent:$002f$002fSD_ASSET$002f0$002fSD_ASSET:1033861/one (accessed on 24 October 2022).
21. Hatjina, F.; Bouga, M. Portrait of *Marchalina hellenica* Gennadius (Hemiptera: Margarodidae), the main producing insect of pine honeydew-biology, genetic variability and honey production. *Bee Sci.* **2009**, *9*, 162–167.
22. Buckley, R.C. Interactions involving plants, Homoptera, and ants. *Annu. Rev. Ecol. Syst.* **1987**, *18*, 111–135. [CrossRef]
23. Zafiri, S.G.; Fasseas, C.P.; Emmanouel, N.G. An approach to the investigation of the *Marchalina hellenica* (Gennadius) (Hemiptera: Margarodidae) in pine. In Proceedings of the 12th Congress of Hellenic Entomological Society, Larnaka, Cyprus, 13–16 November 2007; p. 106.
24. Atkins, C.A.; Smith, P.; Rodriguez-Medina, C. Macromolecules in phloem exudates—A review. *Protoplasma* **2011**, *248*, 165–172. [CrossRef]
25. Quesada, C.R.; Scharf, M.E.; Sadof, C.S. Excretion of non-metabolized insecticides in honeydew of striped pine scale. *Chemosphere* **2020**, *249*, 126167. [CrossRef]
26. Way, M.J. Mutualism between ants and honeydew-producing Homoptera. *Annu. Rev. Entomol.* **1963**, *8*, 307–344. [CrossRef]
27. Ashford, D.A.; Smith, W.A.; Douglas, A.E. Living on a high sugar diet: The fate of sucrose ingested by a phloem-feeding insect, the pea aphid *Acyrthosiphon pisum*. *J. Insect Physiol.* **2000**, *46*, 335–341. [CrossRef] [PubMed]
28. Hodgson, C.; Gounari, S. Morphology of *Marchalina hellenica* (Gennadius) (Hemiptera: Coccoidea: Marchalinidae) from Greece, with a discussion on the identity of *M. caucasica* Hadzibeyli from the Caucasus. *Zootaxa* **2006**, *1196*, 1–32. [CrossRef]
29. Lev-Yadun, S.; Weinstein-Evron, M. The role of *Pinus halepensis* (Aleppo pine) in the landscape of Early Bronze Age Megiddo. *J. Inst. Archaeol. Tel Aviv Univ.* **2002**, *29*, 332–343. [CrossRef]
30. Thrasyvoulou, A.; Manikis, J. Some physicochemical and microscopic characteristics of Greek unifloral honeys. *Apidologie* **1995**, *26*, 441–452. [CrossRef]
31. Bacandritsos, N. Establishment and honeydew honey production of *Marchalina hellenica* (Coccoidea Margarodidae) on fir tree (*Abies cephalonica*). *Bull. Insectology* **2004**, *57*, 127–130.
32. Üglentürk, S.; Szentkirályi, F.; Uygun, N.; Fent, M.; Gaimari, S.D.; Civelek, H.; Ayhan, B. Predators of *Marchalina hellenica* (Hemiptera: Marchalinidae) on pine forests in Turkey. *Phytoparasitica* **2013**, *41*, 529–537.
33. Foldi, I.; Pearce, M.J. Fine structure of wax glands, wax morphology and function in the female scale insect, *Pulvinaria regalis* Canard. (Hemiptera: Coccidae). *Int. J. Insect Morph. Embryol.* **1985**, *14*, 259–271. [CrossRef]
34. Foldi, I. The wax glands in scale insect: Comparative ultrastructure, secretion, function and evolution (Homoptera: Coccoidea). *Ann. Soc. Entomol. Fr.* **1991**, *27*, 163–188.
35. Ahmad, A.; Kundu, A.; Dey, D. Wax glands ultrastructure and chemical composition of wax of giant mealybug *Drosicha stebbingii* (Green) (Hemiptera: Monophlebidae). *J. Asia Pac. Entomol.* **2020**, *23*, 546–553. [CrossRef]

36. Prinzing, A.J. Use of shifting microclimatic mosaics by arthropods on exposed tree trunks. *Ann. Entomol. Soc. Am.* **2001**, *94*, 210–218. [CrossRef]
37. Pincebourde, S.; Casas, J. Warming tolerance across insect ontogeny: Influence of joint shifts in microclimates and thermal limits. *Ecology* **2015**, *96*, 986–997. [CrossRef] [PubMed]
38. Pincebourde, S.; Casas, J. Narrow safety margin in the phyllosphere during thermal extremes. *Proc. Natl. Acad. Sci. USA* **2019**, *116*, 5588–5596. [CrossRef] [PubMed]
39. Chrysopolitou, V.; Apostolakis, A.; Avtzis, D.; Avtzis, N.; Diamandis, S.; Kemitzoglou, D.; Papadimos, D.; Perlerou, C.; Tsiaoussi, V.; Dafis, S. Studies on forest health and vegetation changes in Greece under the effects of climate changes. *Biodivers. Conserv.* **2013**, *22*, 1133–1150. [CrossRef]
40. Christopoulou, A.; Sazeides, C.I.; Fyllas, N.M. Size-mediated effects of climate on tree growth and mortality in Mediterranean Brutia pine forests. *Sci. Total Environ.* **2022**, *812*, 151463. [CrossRef]
41. Dai, A. Increasing drought under global warming in observations and models. *Nat. Clim. Chang.* **2012**, *3*, 52–58. [CrossRef]
42. Wong, C.M.; Daniels, L.D. Novel forest decline triggered by multiple interactions among climate, an introduced pathogen and bark beetles. *Glob. Chang. Biol.* **2017**, *23*, 1926–1941. [CrossRef]
43. Melbourne Water. Victorian Government: Water Storage Levels: Cardinia Reservoir. Available online: https://www.melbournewater.com.au/water-data-and-education/water-storage-levels/water-storage-reservoirs/cardinia (accessed on 22 June 2022).
44. Magnus, G. Versuche über die Spannkräfte des Wasserdampfs. *Ann. Phys.* **1844**, *137*, 225–247. [CrossRef]
45. Alduchov, O.A.; Eskridge, R.E. Improved Magnus form approximation of saturation vapor pressure. *J. Appl. Meteorol.* **1996**, *35*, 601–609. [CrossRef]
46. Lawrence, M.G. The relationship between relative humidity and the dewpoint temperature in moist air: A simple conversion and applications. *Bull. Am. Meteorol. Soc.* **2005**, *86*, 225–234. [CrossRef]
47. Australian Government: Bureau of Meteorology: Climate Data Online. Available online: http://www.bom.gov.au/climate/data/index.shtml (accessed on 25 October 2021).
48. Melbourne Water. Victorian Government: Rainfall and River Levels. Available online: https://www.melbournewater.com.au/water-data-and-education/rainfall-and-river-levels#/reader/586033 (accessed on 25 October 2021).
49. Speight, M.R. The impact of leaf-feeding by nymphs of the horse chestnut scale *Pulvinaria regalis* Canard (Hem. Coccidae), on young host trees. *J. Appl. Entomol.* **1991**, *112*, 389–399. [CrossRef]
50. Gounari, S. Studies on the phenology of *Marchalina hellenica* (gen.) (Hemiptera: Coccoidea, Margarodidae) in relation to honeydew flow. *J. Apic. Res.* **2006**, *45*, 8–12. [CrossRef]
51. Fotelli, M.N.; Lyrou, F.G.; Avtzis, D.N.; Maurer, D.; Rennenberg, H.; Spyroglou, G.; Polle, A.; Radoglou, K. Effective defense of Aleppo Pine against the Giant Scale *Marchalina hellenica* through Ecophysiological and metabolic changes. *Front. Plant Sci.* **2020**, *11*, 581693. [CrossRef]
52. IBM Corp. *IBM SPSS Statistics for Windows*; Version 28.0; IBM Corp: Armonk, NY, USA, 2021.
53. Eleftheriadou, N.; Lubanga, U.; Lefoe, G.; Seehausen, M.L.; Kenis, M.; Kavallieratos, N.G.; Avtzis, D.N. Phenology and potential fecundity of *Neoleucopis kartliana* in Greece. *Insects* **2022**, *13*, 143. [CrossRef] [PubMed]
54. Dunnett, C.W. Pairwise multiple comparisons in the unequal variance case. *J. Am. Stat. Assoc.* **1980**, *75*, 796–800. [CrossRef]
55. Abdi, H.; Williams, L.J. Tukey's honestly significant difference (HSD) test. *Ency. Res. Des.* **2010**, *3*, 1–5.
56. Durbin, J.; Watson, G.S. Testing for serial correlation in least squares regression III. *Biometrika* **1971**, *58*, 1–19. [CrossRef]
57. White, K.J. The Durbin-Watson test for autocorrelation in nonlinear models. *Rev. Econ. Stat.* **1992**, *74*, 370–373. [CrossRef]
58. Bacandritsos, N.; Saitanis, C.; Papanastasiou, I. Morphology and life cycle of *Marchalina hellenica* (Gennadius) (Hemiptera: Margarodidae) on pine (Parnis Mt.) and fir (Helmos Mt.) forests of Greece. *Ann. Soc. Entomol. Fr.* **2004**, *40*, 169–176. [CrossRef]
59. Petrakis, P.V.; Roussis, V.; Vagias, C.; Tsoukatou, M. The interaction of pine scale with pines in Attica, Greece. *Eur. J. For. Res.* **2010**, *129*, 1047–1056. [CrossRef]
60. Álvarez, J.; Allen, H.L.; Albaugh, T.J.; Stape, J.L.; Bullock, B.P.; Song, C. Factors influencing the growth of radiata pine plantations in Chile. *Forestry* **2013**, *86*, 13–26. [CrossRef]
61. Saremi, H.; Kumar, L.; Turner, R.; Stone, C.; Melville, G. DBH and height show significant correlation with incoming solar radiation: A case study of a radiata pine (*Pinus radiata* D. Don) plantation in New South Wales, Australia. *GISci. Remote Sens.* **2014**, *5*, 427–444. [CrossRef]
62. White, T.C.R. The abundance of invertebrate herbivores in relation to the availability of nitrogen in stressed food plants. *Oecologia* **1984**, *63*, 90–105. [CrossRef]
63. White, T.C.R. Are outbreaks of cambium-feeding beetles generated by nutritionally enhanced phloem of drought-stressed trees? *J. Appl. Entomol.* **2014**, *139*, 567–578. [CrossRef]
64. Sperry, J.S.; Love, D.M. What plant hydraulics can tell us about responses to climate-change droughts. *New Phytol.* **2015**, *207*, 14–27. [CrossRef]
65. Sevanto, S. Drought impacts on phloem transport. *Curr. Opin. Plant Biol.* **2018**, *43*, 76–81. [CrossRef]
66. Petrakis, P.V.; Spanos, K.; Feest, A. Insect biodiversity reduction of pinewoods in southern Greece caused by the pine scale (*Marchalina hellenica*). *For. Syst.* **2011**, *20*, 27–41. [CrossRef]

67. Avtzis, D.N.; Lubanga, U.K.; Lefoe, G.K.; Kwong, R.M.; Eleftheriadou, N.; Andreadi, A.; Elms, S.; Shaw, R.; Marc, K. Prospects for classical biocontrol of *Marchalina hellenica* in Australia. *Biocontrol* **2020**, *65*, 413–423. [CrossRef]
68. Wolfe, L.M. Why alien invaders succeed: Support for the escape-from-enemy hypothesis. *Am. Nat.* **2002**, *160*, 705–711. [CrossRef]
69. Colautti, R.I.; Ricciardi, A.; Grigorovich, I.A.; MacIsaac, H.J. Is invasion success explained by the enemy release hypothesis? *Ecol. Lett.* **2004**, *7*, 721–733. [CrossRef]
70. Meijer, K.; Schilthuizen, M.; Beukeboom, L.; Smit, C. A review and meta-analysis of the enemy release hypothesis in plant-herbivorous insect systems. *PeerJ* **2016**, *4*, e2778. [CrossRef] [PubMed]
71. Duan, J.J.; Van Driesche, R.G.; Crandall, R.S.; Schmude, J.M.; Rutledge, C.E.; Slager, B.H.; Gould, J.R.; Elkinton, J.S. Establishment and early impact of *Spathius galinae* (Hymenoptera: Braconidae) on emerald ash borer (Coleoptera: Buprestidae) in the Northeastern United States. *J. Econ. Entomol.* **2019**, *112*, 2121–2130. [CrossRef]
72. Weinstein-Evron, M.; Lev-Yadun, S. Palaeoecology of *Pinus halepensis* in Israel in the Light of Archeobotanical Data. In *Ecology, Biogeography and Management of Pinus halepensis and Pinus brutia Forest Ecosystems in the Mediterranean Basin*; Ne'eman, G., Trabaud, L., Eds.; Backhuys Publishers: Leiden, The Netherlands, 2000; pp. 119–130.
73. Mita, E.; Tsitsimpikou, C.; Tsiveleka, L.; Petrakis, P.V.; Oritz, A.; Vagias, C.; Roussis, V. Seasonal variation of oleoresin terprenoids from *Pinus halepensis* and *Pinus pinea* and host selection of the scale insect *Marchalina hellenica* (Homoptera, Coccoidea, Margarodidae, Coelostonidiinae). *Holzforschung* **2002**, *56*, 572–578. [CrossRef]
74. Anderegg, W.R.L.; Hicke, J.A.; Fisher, R.A.; Allen, C.D.; Aukema, J.; Bentz, B.; Hood, S.; Lichstein, J.W.; Macalady, A.K.; McDowell, N.; et al. Tree mortality from drought, insects, and their interactions in a changing climate. *New Phytol.* **2015**, *208*, 674–683. [CrossRef] [PubMed]
75. Chen, L.; Huan, J.; Dawson, A.; Zhai, L.; Stadt, K.J.; Comeau, P.G.; Whitehouse, C. Contributions of insects and droughts to growth decline of trembling aspen mixed boreal forest of western Canada. *Glob. Chang. Biol.* **2017**, *24*, 655–667. [CrossRef]
76. Raderschall, C.A.; Vico, G.; Lundin, O.; Taylor, A.R.; Bommarco, R. Water stress and insect herbivory interactively reduce crop yield while the insect pollination benefit is conserved. *Glob. Chang. Biol.* **2020**, *27*, 71–83. [CrossRef]
77. Honek, A.; Martinkova, Z.; Pekár, S. How climate changes affects the occurrence of a second generation in the univoltine *Pyrrhocoris apterus* (Heteroptera: Pyrrhocoridae). *Ecol. Entomol.* **2020**, *45*, 1172–1179. [CrossRef]
78. Awmack, C.S.; Leather, S.R. Host plant quality and fecundity in herbivorous insects. *Annu. Rev. Entomol.* **2002**, *47*, 817–844. [CrossRef]
79. Hale, B.K.; Bale, J.S.; Pritchard, J.; Masters, G.J.; Brown, V.K. Effects of host plant drought stress on the performance of the bird cherry-oat aphid, *Rhopalosiphum padi* (L.): A mechanistic analysis. *Ecol. Entomol.* **2003**, *2896*, 666–677. [CrossRef]
80. Huberty, A.F.; Denno, R. Plant water stress and its consequences for herbivorous insects: A new synthesis. *Ecology* **2004**, *85*, 1383–1398. [CrossRef]
81. Tariq, M.; Wright, D.J.; Rossiter, J.T.; Staley, J.T. Aphids in a changing world: Testing the plant stress, plant vigour and pulsed stress hypothesis. *Agric. For. Entomol.* **2012**, *14*, 177–185. [CrossRef]
82. Akoh, J.I.; Aigbodion, F.I.; Kumbak, D. Studies on the effect of larval diet, adult body weight, size of blood-meal and age on the fecundity of *Culex quinquefasciatus* (Diptera: Culicidae). *Int. J. Trop. Insect Sci.* **1992**, *13*, 177–181. [CrossRef]
83. Aluja, M.; Díaz-Fleischer, F.; Papaj, D.R.; Lagunes, G.; Sivinski, J. Effects of age, diet, female density, and the host resource on egg load in *Anastrepha ludens* and *Anastrepha obliqua* (Diptera: Tephritidae). *J. Insect Physiol.* **2001**, *47*, 975–988. [CrossRef] [PubMed]
84. Mitchell, P.K.; O'Grady, A.P.; Tissue, D.T.; White, D.A.; Ottenschlaeger, M.L.; Pinkard, E.A. Drought response strategies define the relative contributions of hydraulic dysfunction and carbohydrate depletion during tree mortality. *New Phytol.* **2012**, *197*, 862–872. [CrossRef]
85. Caird, M.A.; Richards, J.H.; Donovan, L.A. Nighttime stomatal conductance and transpiration in C3 and C4 plants. *Plant Physiol.* **2007**, *143*, 4–10. [CrossRef] [PubMed]
86. Ungar, E.D.; Rotenberg, E.; Raz-Yaseef, N.; Cohen, S.; Yakir, D.; Schiller, G. Transpiration and annual water balance of Aleppo pine in a semiarid region: Implications for forest management. *For. Ecol. Manag.* **2013**, *298*, 39–51. [CrossRef]
87. Steppe, K.; Sterck, F.; Deslauriers, A. Diel growth dynamics in tree stems: Linking anatomy and ecophysiology. *Trends Plant Sci.* **2015**, *20*, 335–343. [CrossRef]
88. Salazar-Tortosa, D.; Castro, J.; Villar-Salvador, P.; Viñegla, B.; Matías, L.; Michelsen, A.; De Casas, R.R.; Querejeta, J.I. The "isohydric trap": A proporsed feedback between water shortage, stomatal regulation, and nutrient acquisition drives differential growth and survival of European pines under climatic dryness. *Glob. Chang. Biol.* **2018**, *24*, 4069–4083. [CrossRef]
89. Blackman, C.J.; Creek, D.; Maier, C.; Aspinwall, M.J.; Drake, J.E.; Pfautsch, S.; O'Grady, A.; Delzon, S.; Medlyn, B.E.; Tissue, D.T.; et al. Drought response strategies and hydraulic traits contribute to mechanistic understanding of plant dry-down to hydraulic failure. *Tree Physiol.* **2019**, *39*, 910–924. [CrossRef]
90. Gould, N.; Thorpe, M.R.; Koroleva, O.; Minchin, P.E.H. Phloem hydrostatic pressure relates to solute loading rate: A direct test for the Münich hypothesis. *Funct. Plant Biol.* **2005**, *32*, 1019–1026. [CrossRef]
91. Hamann, E.; Blevins, C.; Franks, S.J.; Jameel, M.I.; Anderson, J.T. Climate change alters plant-herbivore interactions. *New Phytol.* **2020**, *229*, 1894–1910. [CrossRef] [PubMed]